

How Deep is the Antinucleon Optical Potential at FAIR energies

T. Gaitanos, M. Kaskulov, H. Lenske

Institut für Theoretische Physik, Universität Giessen, Heinrich-Buff-Ring 16, 35392 Giessen, Germany

Abstract

The key question in the interaction of antinucleons in the nuclear medium concerns the deepness of the antinucleon-nucleus optical potential. In this work we study this task in the framework of the non-linear derivative (NLD) model which describes consistently bulk properties of nuclear matter and Dirac phenomenology of nucleon-nucleus interactions. We apply the NLD model to antinucleon interactions in nuclear matter and find a strong decrease of the vector and scalar self-energies in energy and density and thus a strong suppression of the optical potential at zero momentum and, in particular, at FAIR energies. This is in agreement with available empirical information and, therefore, resolves the issue concerning the incompatibility of G-parity arguments in relativistic mean-field (RMF) models. We conclude the relevance of our results for the future activities at FAIR.

Keywords: relativistic hadrodynamics, non-linear derivative model, nuclear matter, Schrödinger equivalent optical potential, proton-nucleus optical potential, antiproton-nucleus optical potential

1. Introduction

The in-medium nucleon-nucleon interaction has been an object of intensive theoretical and experimental research of modern nuclear physics over the last few decades, see for a review [1]. The main finding was a softening of the nuclear equation of state at densities reached in intermediate energy nucleus-nucleus collisions, which was consistent with a variety of phenomenological [2] and microscopic [3] models. In addition the empirical saturation of the proton-nucleus optical potential turned out to be consistent with heavy-ion theoretical studies [4].

While the bare antinucleon-nucleon ($\bar{N}N$) interaction has been actively studied, see Refs. [5] and references therein, empirical information on the in-medium interactions of antinucleons is still very poor. Antiproton production has been investigated theoretically in reactions induced by protons [6] and heavy ions in the SIS-energy region [7], where some data on antiprotons were available. Complementary studies of antiproton annihilation in nuclei [8] and antiprotonic atoms [9] provided further insight on the optical potential at very low energies, however, with rather big uncertainties in the nuclear interior due to the strong annihilation cross section at the surface of the nucleus.

In the near future the FAIR facility intends to study the still controversial and empirically less known high energy domain of the (anti)nuclear interactions in more details

than before. For instance, the nuclear equation of state for strangeness degrees of freedom and also the in-medium antinucleon-nucleon interaction are some of the key projects [10]. They are relevant for the formation of exotic (anti)matter systems such as double-strange hypernuclei and $\bar{\Lambda}$ -hypernuclei in antiproton-induced reactions in the \bar{P} ANDA experiment at FAIR [11].

The microscopic Brueckner-Hartree-Fock calculations of the in-medium $\bar{N}N$ -scattering have been carried out in [12]. On the other hand, a complementary theoretical background for phenomenological models builds the relativistic hadrodynamics (RHD). It is based on the relativistic mean-field (RMF) theory, which is a well established tool for infinite and finite nuclear systems [13]. However, as already shown many years ago [7], there are still unresolved problems in RMF models, when applying them to antiproton-nucleus scattering and to heavy ion collisions. By just imposing G-parity arguments, like in microscopic models [12, 14], the RMF do not describe the experimental data [7, 15, 16]. This incompatibility of mean-field models with respect to G-parity symmetry has been also shown in recent transport studies [15], where one had to largely decrease the antinucleon-meson couplings by hand in order to reproduce the empirical data.

In this work we address this issue why the conventional RMF models do not describe antiproton-nucleus Dirac phenomenology. To be more specific, our studies are based on the non-linear derivative (NLD) model [17] to RMF. The NLD model describes simultaneously the density dependence of the nuclear equation of state and the energy dependence of the proton-nucleus optical potential. Latter feature is missing in standard RMF models. Then applying G-parity transformation it is shown that the real part of the proton *and simultaneously* the real part of the antiproton optical potentials are reproduced fairly well in comparison with phenomenological studies. We finally make predictions for the deepness of the real part of the antiproton optical potential and estimate its imaginary part at low energies and energies relevant for the forthcoming experiments at FAIR.

2. NLD formalism

The NLD approach [17] to nuclear matter is based essentially on the Lagrangian density of RHD [13]. It describes the interaction of nucleons through the exchange of auxiliary meson fields (Lorentz-scalar, σ , and Lorentz-vector meson fields ω^μ) [18]

$$\mathcal{L} = \mathcal{L}_{Dirac} + \mathcal{L}_{mes} + \mathcal{L}_{int} . \quad (1)$$

The Lagrangian in Eq. (1) consists of the free Lagrangians for the Dirac field Ψ and for the meson fields σ and ω^μ . The isovector meson ρ is not considered here, for simplicity.

In conventional RHD the interaction Lagrangian \mathcal{L}_{int} contains meson fields which couple to the Dirac field via the corresponding Lorentz-density operators $g_\sigma \bar{\Psi}\Psi\sigma$ and $-g_\omega \bar{\Psi}\gamma^\mu\Psi\omega_\mu$ for the scalar and vector parts, respectively. Such interactions describe rather successfully the saturation properties of nuclear matter, but they miss the energy dependence of the mean field. A possible solution to this problem has been proposed in [6] where the momentum-dependent phenomenological form factors were introduced. In [17] this

idea has been generalized in a manifestly covariant way. In particular, the symmetrized interaction in the NLD model is given by

$$\mathcal{L}_{int} = \frac{g_\sigma}{2} \left[\overline{\Psi} \overleftarrow{\mathcal{D}} \Psi \sigma + \sigma \overline{\Psi} \overrightarrow{\mathcal{D}} \Psi \right] - \frac{g_\omega}{2} \left[\overline{\Psi} \overleftarrow{\mathcal{D}} \gamma^\mu \Psi \omega_\mu + \omega_\mu \overline{\Psi} \gamma^\mu \overrightarrow{\mathcal{D}} \Psi \right]. \quad (2)$$

The interaction between the Dirac and the meson fields has a similar functional form as in standard RHD [13]. However, now new operators \mathcal{D} acting on the nucleon fields appear, which are the non-linear functionals of partial derivatives

$$\overrightarrow{\mathcal{D}} := \exp \left(\frac{-v^\beta i \overrightarrow{\partial}_\beta + m}{\Lambda} \right), \quad \overleftarrow{\mathcal{D}} := \exp \left(\frac{i \overleftarrow{\partial}_\beta v^\beta + m}{\Lambda} \right). \quad (3)$$

In Eq. (3) v^β denotes a dimensionless auxiliary 4-vector and Λ stands for the cut-off parameter. The latter has been adjusted to the saturation properties of nuclear matter [17]. In the limiting case of $\Lambda \rightarrow \infty$ the standard Walecka model is retained.

The NLD Lagrangian \mathcal{L} is a functional of not only Ψ , $\overline{\Psi}$ and their first derivatives, but it depends on all higher order covariant derivatives of Ψ and $\overline{\Psi}$. For such a generalized functional the Euler-Lagrange equations take the form [17]

$$\begin{aligned} \frac{\partial \mathcal{L}}{\partial \phi} - \partial_{\alpha_1} \frac{\partial \mathcal{L}}{\partial (\partial_{\alpha_1} \phi)} + \partial_{\alpha_1} \partial_{\alpha_2} \frac{\partial \mathcal{L}}{\partial (\partial_{\alpha_1} \partial_{\alpha_2} \phi)} + \dots + \\ (-)^n \partial_{\alpha_1} \partial_{\alpha_2} \dots \partial_{\alpha_n} \frac{\partial \mathcal{L}}{\partial (\partial_{\alpha_1} \partial_{\alpha_2} \dots \partial_{\alpha_n} \phi)} = 0. \end{aligned} \quad (4)$$

Contrary to the standard expressions for the Euler-Lagrange equation, now infinite series of terms ($n \rightarrow \infty$) proportional to higher order derivatives of the Dirac field ($\phi = \Psi, \overline{\Psi}$) appear. They can be evaluated by a Taylor expansion of the non-linear derivative operators (3). As shown in [17], in nuclear matter an infinite series of terms can be resummed exactly and the following Dirac equation is obtained

$$[\gamma_\mu (i \partial^\mu - \Sigma^\mu) - (m - \Sigma_s)] \Psi = 0, \quad (5)$$

with Lorentz-vector and Lorentz-scalar self-energies defined as follows

$$\Sigma^\mu = g_\omega \omega^\mu e^{\frac{-v^\beta i \overrightarrow{\partial}_\beta + m}{\Lambda}}, \quad \Sigma_s = g_\sigma \sigma e^{\frac{-v^\beta i \overrightarrow{\partial}_\beta + m}{\Lambda}}. \quad (6)$$

The Proca and Klein-Gordon equations for the meson fields can be also derived

$$\partial_\mu F^{\mu\nu} + m_\omega^2 \omega^\nu = \frac{1}{2} g_\omega \left[\overline{\Psi} e^{\frac{i \overleftarrow{\partial}_\beta v^\beta + m}{\Lambda}} \gamma^\nu \Psi + \overline{\Psi} \gamma^\nu e^{\frac{-v^\beta i \overrightarrow{\partial}_\beta + m}{\Lambda}} \Psi \right], \quad (7)$$

$$\partial_\mu \partial^\mu \sigma + m_\sigma^2 \sigma = \frac{1}{2} g_\sigma \left[\overline{\Psi} e^{\frac{i \overleftarrow{\partial}_\beta v^\beta + m}{\Lambda}} \Psi + \overline{\Psi} e^{\frac{-v^\beta i \overrightarrow{\partial}_\beta + m}{\Lambda}} \Psi \right], \quad (8)$$

with the field tensor $F^{\mu\nu} = \partial^\mu \omega^\nu - \partial^\nu \omega^\mu$. The meson field equations (7) and (8) show a similar form as in the linear Walecka model of RHD, except of the highly non-linear

behavior of the source terms, which generate selfconsistent couplings between the meson-field equations.

Applying the usual RMF approximation to the idealized system of infinite nuclear matter, the Dirac equation (5) maintains its original form. However, we have to distinguish between nucleons (N) forming the nuclear matter and antinucleons (\bar{N}) which interact with the nuclear matter. For the description of antiparticles we require G-parity invariance of the Dirac equation and then follow the standard procedure of applying a G-parity transformation $G = Ce^{i\pi I_2}$ to the negative energy states, where I_2 is the operator associated with the 2nd component of the isospin "vector" and C is the charge conjugation operator. The invariance of the Dirac equation under charge conjugation requires that the auxiliary vector v^β must be odd under C-parity transformation. With our choice of $v^\beta = (1, \vec{0})$ for positive energy solutions [17] this results in $v^\beta = (-1, \vec{0})$ for the charge conjugated Dirac field. This leads to the following Dirac equations for nucleons

$$[\gamma_\mu(i\partial^\mu - \Sigma^\mu) - (m - \Sigma_s)] \Psi_N = 0 \quad (9)$$

and antinucleons

$$[\gamma_\mu(i\partial^\mu + \Sigma^\mu) - (m - \Sigma_s)] \Psi_{\bar{N}} = 0 \quad (10)$$

interacting with nuclear matter, where $\Psi_N = \Psi^+$ and $\Psi_{\bar{N}} = \Psi_C$ denote the positive energy and the charge conjugated Dirac fields, respectively.

The nucleon and antinucleon self-energies entering Eqs. (9) and (10) are the same

$$\begin{aligned} \Sigma_v \equiv \Sigma^0 &= g_\omega \omega_0 e^{-\frac{E-m}{\Lambda}}, \\ \Sigma_s &= g_\sigma \sigma e^{-\frac{E-m}{\Lambda}}. \end{aligned} \quad (11)$$

However, note the opposite signs in the Lorentz-vector interactions in Eqs. (9) and (10). Furthermore, the single particle energies E have to be obtained from the in-medium mass-shell conditions which are different for nucleons (N) and antinucleons (\bar{N})

$$E_N(p) = \sqrt{p^2 + m^{*2}} + \Sigma_v, \quad E_{\bar{N}}(p) = \sqrt{p^2 + m^{*2}} - \Sigma_v. \quad (12)$$

The in-medium (or effective) Dirac mass in Eq. (12) is given by $m^* = m - \Sigma_s$. Note, that m^* depends explicitly on particle momentum. Again, in the limiting case of $\Lambda \rightarrow \infty$, the exponential factor is equal to unity and the equations are reduced to the ones from the Walecka model. In the NLD model the cut-off parameter Λ is of natural size, i.e., of typical hadronic mass scale in this problem. In the following, $\Lambda = 770$ MeV is chosen, as in the original work [17].

In nuclear matter the NLD equations of motion for ω and σ simplify to standard algebraic equations

$$m_\omega^2 \omega^0 = g_\omega \rho_v, \quad m_\sigma^2 \sigma = g_\sigma \rho_s \quad (13)$$

with the corresponding density sources $\rho_v = \langle \bar{\Psi}_N \gamma^0 e^{-\frac{E-m}{\Lambda}} \Psi_N \rangle$ and $\rho_s = \langle \bar{\Psi}_N e^{-\frac{E-m}{\Lambda}} \Psi_N \rangle$. The vector density ρ_v is not related to the conserved nucleon density ρ . It has to be derived

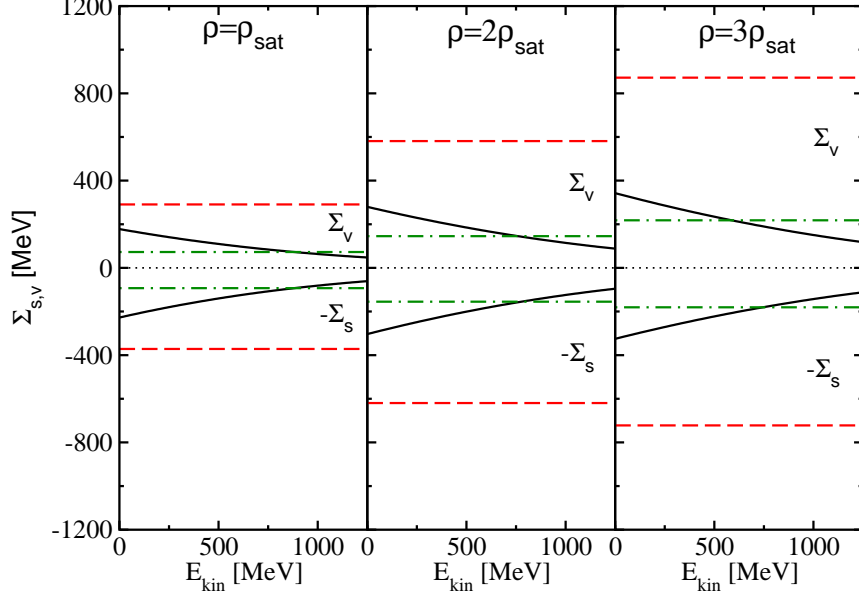


Figure 1: Kinetic energy dependence of the scalar and vector Lorentz-components of the antinucleon self-energy in nuclear matter at densities of $\rho = \rho_{\text{sat}}$ (left), $\rho = 2\rho_{\text{sat}}$ (middle) and $\rho = 3\rho_{\text{sat}}$ (right) using the linear Walecka model (dashed lines), the linear Walecka model with rescaled couplings with the factor $\xi = 0.25$ [15] (dash-dotted) and the NLD approach (solid lines).

from a generalized Noether-theorem [17] and reads

$$J^0 \equiv \rho = \langle \bar{\Psi}_N \gamma^0 \Psi_N \rangle + \frac{g_\omega}{\Lambda} \langle \bar{\Psi}_N \gamma^0 e^{-\frac{E-m}{\Lambda}} \Psi_N \rangle \omega_0 - \frac{g_\sigma}{\Lambda} \langle \bar{\Psi}_N e^{-\frac{E-m}{\Lambda}} \Psi_N \rangle \sigma \quad . \quad (14)$$

The meson-nucleon couplings g_ω and g_σ can be taken from any linear Walecka model, e.g., [13], as it has been done here. Moreover, we use the same coupling constants for both nucleon and antinucleon interactions.

3. Results and Discussion

We have applied both the NLD and the conventional linear Walecka models to nuclear matter at various baryon densities and also at various nucleon and antinucleon energies relative to matter at rest. At first, we discuss the self-energies, which are real quantities in RMF. Then we focus our study on the energy and density dependencies of the optical potential, first for in-medium proton interactions, and then for the antiproton case.

Fig. 1 shows the Lorentz-scalar and Lorentz-vector components of the antinucleon self-energy in nuclear matter, Σ_s and Σ_v , as a function of the kinetic energy at three baryon densities. The antinucleon kinetic energy is calculated relative to the potential depth of the nuclear matter at rest, i.e., $E_{\text{kin}} = E_{\bar{N}} - m = \sqrt{p^2 + m^{*2}} - \Sigma_v - m$. The NLD calculations show an explicit energy dependence for both components of the antinucleon self-energy. In particular, the self-energies decrease with increasing energy, for all baryon densities. On the other hand, with rising baryon density they increase only moderately at each

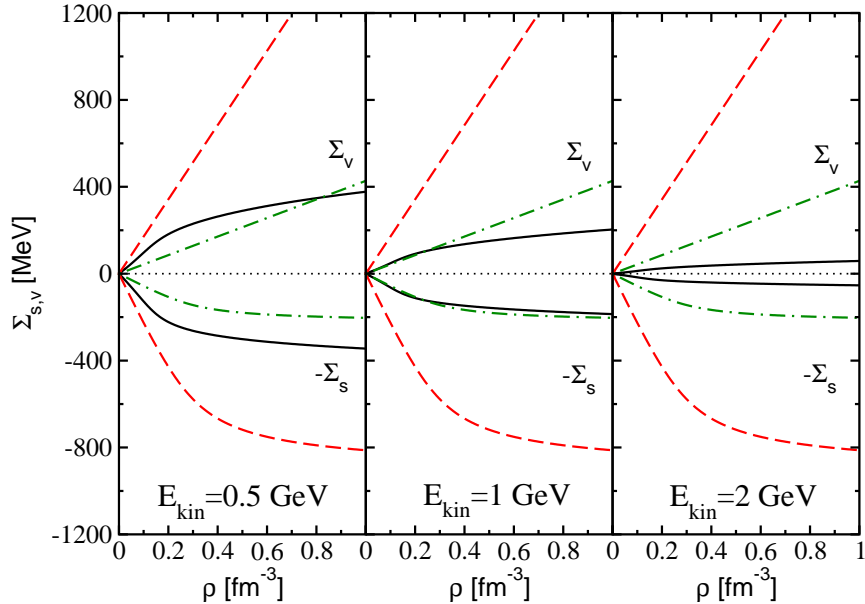


Figure 2: Density dependence of the scalar and vector Lorentz-components of the antinucleon self-energy in nuclear matter at energies of $E_{\text{kin}} = 0.5$ GeV (left), $E_{\text{kin}} = 1$ GeV (middle) and $E_{\text{kin}} = 2$ GeV (right) using the linear Walecka model (dashed lines), the linear Walecka model with rescaled couplings with the factor $\xi = 0.25$ [15] (dash-dotted) and the NLD approach (solid lines).

energy. The saturation in energy and density results from the non-linear interaction, as discussed in detail in Ref. [17]. In the linear Walecka model the Lorentz-vector self-energy grows strongly with increasing density, while the Lorentz-scalar component saturates. Both components in the standard RMF are energy independent.

For antinucleon interactions in nuclear matter the mean-field potential consists of the sum of scalar and vector self-energies. At vanishing momentum and at saturation density the linear Walecka model leads to a value of $-\Sigma_v - \Sigma_s \approx -700$ MeV, which is too deep according to phenomenology [19, 20]. This feature has been always a critical problem in standard RMF models. Even the inclusion of non-linear self-interactions of the σ field (and eventually of the ω field) [21] do not improve the result, since non-linear self-interactions become pronounced only above the saturation density. On the other hand, the NLD model reduces considerably the deepness of the potential at zero momentum by almost a factor of two. The particular difference of the potential depth at vanishing momentum between conventional RMF and NLD is not a trivial issue. The consequences of such an energy and density behavior will be discussed below when considering the optical potentials.

As discussed in Ref. [15], in order to reproduce the data from antiproton-induced reactions, the antinucleon-meson coupling constants of the Walecka model have to be rescaled by a factor of $\xi \simeq 0.2 - 0.3$. Fig. 1 shows also the calculations in the linear Walecka model, but with rescaled couplings by a factor of $\xi = 0.25$ (dash-dotted curves in Fig. 1). Indeed, as one can see in Fig. 1, the rescaled Walecka model [15] reproduces the NLD results in average. However, former results fail to reproduce the energy dependence and, in particular,

the density dependence, as it is demonstrated in Fig. 2. In Fig. 2 the density dependence (at various fixed kinetic energies) of the antinucleon self-energies is displayed. The NLD self-energies saturate with density and energy according to microscopic Dirac-Brueckner studies, as discussed in detail in [17]. In the conventional Walecka model the vector self-energy diverges with increasing density leading to a too strong repulsion at high densities. In fact, this effect of repulsive nature is softened in the rescaled model to large extent, however, the linear divergent behavior of the vector self-energy still remains. The NLD calculations agree (in average) with the rescaled Walecka model around the saturation density and at kinetic energies around 1 GeV only.

The very different energy behavior of the self-energies between NLD and linear Walecka models influences the Schrödinger-equivalent optical potential. In general, it is extracted from (anti)proton-nucleus scattering and therefore it is suited for comparisons between theory and empirical studies. Its real part is given by

$$\Re U_{\text{opt}} = \pm \frac{E}{m} \Sigma_v - \Sigma_s + \frac{1}{2m} (\Sigma_s^2 - \Sigma_v^2) , \quad (15)$$

where E is the energy of an (anti)nucleon with bare mass m inside nuclear matter at a fixed baryon density and upper (lower) sign holds for nucleons (antinucleons). At first we consider the proton-nucleus optical potential.

Fig. 3 shows the real part of the optical potential according to Eq. (15) as function of the nucleon kinetic energy $E_{kin} = E - m = \sqrt{p^2 + m^{*2}} + \Sigma_v - m$. The linear Walecka model (dashed curve) predicts the behavior of the optical potential versus energy only qualitatively, and strongly diverges with increasing kinetic energy of the nucleon. It does not reproduce the empirical saturation at higher energies. This problem is well known in RMF and has already attracted much attention in the past [23]. Of course, the main reason for such strong deviation is the missing energy dependence of the self-energy in the standard RMF. As discussed in detail in Ref. [17], the NLD approach resolves this issue of RMF models. The solid curve in Fig. 3 corresponds to the NLD calculations and describes the data very well.

On the other hand, the interaction of an antinucleon at a given momentum relative to nuclear matter at rest is quite different with respect to the proton-nucleus interaction: the sign of the Lorentz-vector self-energy changes in Eq. (15). Therefore, in the linear Walecka model the real part of the optical potential is again a linear function in energy, as in the nucleon case, but now it diverges to $-\infty$ (see Fig. 4, dashed curve). Such a prediction is in contradiction with calculations using dispersion relations [7]. In fact, by fitting the imaginary part of the antinucleon-nucleus optical potential to the total proton-antiproton cross section, its real part decreases with increasing energy. Furthermore, an existing information from heavy-ion collisions [7] and reactions induced by protons [7] and antiprotons [15] give clear evidence for a considerable reduction of the antiproton-nucleus optical potential with rising energy. As has been discussed in Ref. [15], the transport theoretical description of antiproton-nucleus data is not possible within the conventional Walecka model, except if one rescales the antinucleon-meson coupling constants by a phenomenological factor of $\xi \approx 0.2$. This is not compatible with G-parity arguments and suggests a strong violation

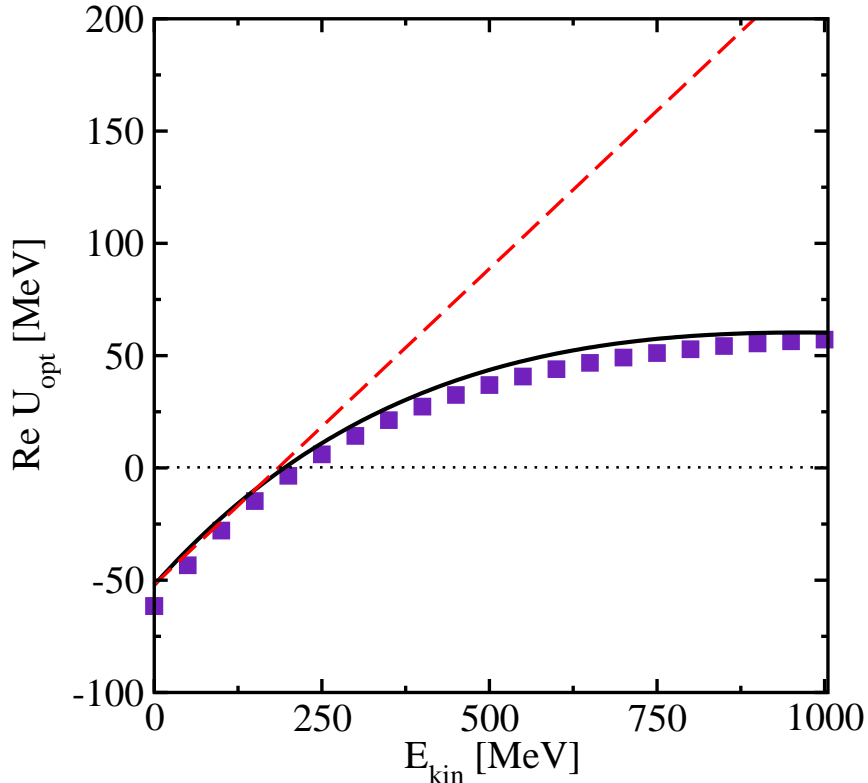


Figure 3: Energy dependence of the Schrödinger equivalent proton optical potential at saturation density $\rho_{sat} = 0.16 \text{ fm}^{-3}$. Theoretical calculations in the linear Walecka model (dashed) and NLD approach (solid) are compared to Dirac phenomenology [22].

of the charge conjugation symmetry in the nuclear medium [16], which otherwise must be a perfect symmetry in strong interactions.

On the contrary, the NLD calculations (solid curve in Fig. 4) predict a completely different behavior as compared with the Walecka model. It results in a much softer potential at vanishing momentum and much stronger decrease of the real part of the optical potential $\Re U_{opt}$ with increasing energy.

Due to the large annihilation cross section experimental data at low energies can be obtained only at very low densities $\rho \simeq (0.005 \div 0.02)\rho_{sat}$ close to the nuclear surface [19, 20], while empirical information at saturation density is obtained by extrapolation only. At these low densities the NLD model leads to values of $\Re U_{opt} \simeq -(6 \div 50) \text{ MeV}$, which seem to be still too deep with respect to the data [19, 20]. At the density of interest $\rho = \rho_{sat}$ the NLD model predicts a rather soft potential, which is much closer to extrapolated data [19, 20] and dispersion relations [7] (filled box at zero kinetic energy in Fig. 4). A comparison between our model and phenomenological antiproton-nucleus reactions at higher energies seems more meaningful. In fact, with increasing energy the annihilation cross section drops strongly and it is supposed that the antiprotons may penetrate deeper inside the nuclear interior, and thus densities close to ρ_{sat} can be tested. The second

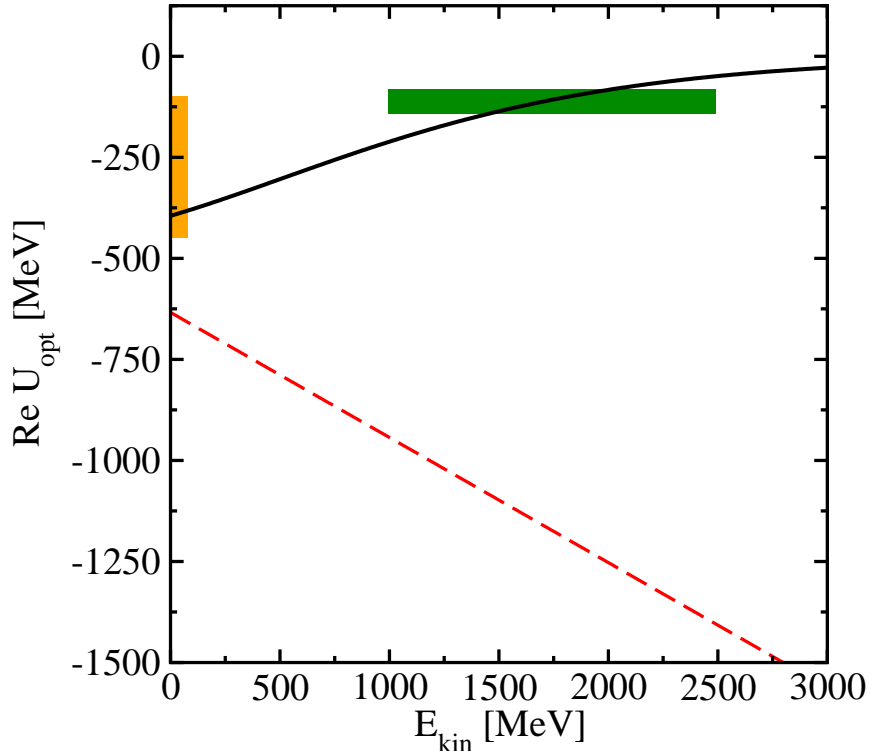


Figure 4: Same as Fig. 3, but for the antiproton case. The filled box at vanishing momentum represents empirical data extrapolated to saturation density [19]. The second filled area at kinetic energies between 1000 and 2500 MeV is taken from transport calculations on antiproton-nucleus reactions [15].

filled area in Fig. 4 shows the empirical optical potential as extracted from the transport theoretical analyses in Ref. [15, 24]. In this energy region the comparison between NLD results and transport calculations (which use conventional RMF, but with largely reduced antinucleon-meson couplings) turns out to be fairly well. Our results are also in qualitative agreement with the analysis of Ref. [25], where a strong decrease of $\Re U_{\text{opt}}$ with increasing energy is obtained.

Interestingly, the antinucleon optical potentials $\Re U_{\text{opt}}$ strongly differ at zero momentum between NLD and standard RMF, while in the nucleon case (see Fig. 3) no differences were visible. By considering the fields at the same baryon density and at zero momentum one would naively expect a similar potential depth for both models. Indeed, the non-linear effects start to dominate above the saturation density [17]. However, the observed difference at zero momentum comes from the in-medium dependence of the (anti)nucleon single-particle energy. At fixed saturation density the energy shift, caused by the difference (proton-nucleus) or sum (antiproton-nucleus) of two big fields, varies strongly between the two models. However, small shift variations in the energy affect the NLD self-energies, due to their pronounced energy dependence. On the other hand, the fields of the linear Walecka model are not influenced due to their independence on energy. This feature becomes more pronounced with increasing density, as seen in Fig. 1 (middle and right panels). In terms

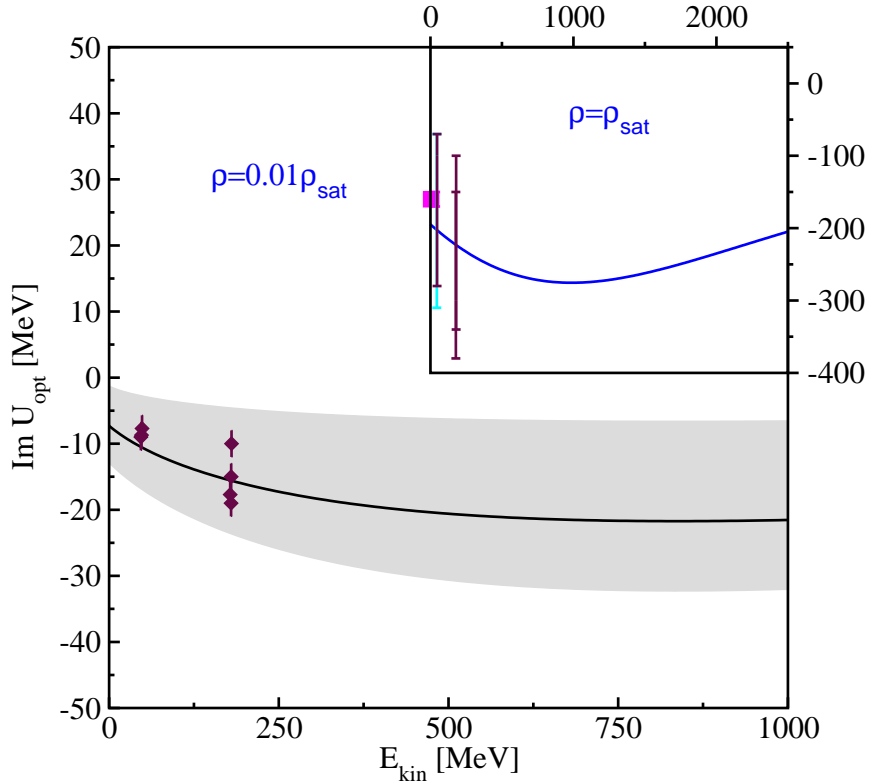


Figure 5: Energy dependence of the imaginary part of the antinucleon optical potential at low density, as indicated. The theoretical result, extracted from the dispersion relation (see Eq. (16)) in the NLD approach (solid curves) is compared to experimental data (symbols) taken from [20]. The filled area indicates the model changes by varying the density from 0.005 up to 0.02 (relative to ρ_{sat}). The inserted panel shows the same quantity but at the fixed saturation density $\rho_{sat} = 0.16 \text{ fm}^{-3}$, again in comparison to data (symbols), which are extrapolated to ρ_{sat} .

of the optical potentials the interpretation is similar. In the proton-nucleus case (Fig. 3) the slopes between both models at vanishing momentum are essentially the same. Therefore the in-medium energy shift is of minor relevance and there is no gap between both potentials. In the antiproton-nucleus case (Fig. 4) the gap is much more pronounced due to the quite different slopes between NLD and linear Walecka optical potentials.

For a complete description of in-medium antiproton interactions also the imaginary part of the optical potential is needed. Since RMF does not provide the imaginary part of the self-energies, we estimate $\Im m U_{opt}$ using dispersion relation [26]

$$\Im m U_{opt}(p) = -\frac{2p}{\pi} \mathcal{P} \int_0^\infty \frac{\Re e U_{opt}(p')}{p'^2 - p^2} dp', \quad (16)$$

where $p \equiv |\vec{p}|$ means the antiparticle momentum and \mathcal{P} denotes the principal value. The real part $\Re e U_{opt}$ is taken from the NLD model. The results are shown in Fig. 5. The insert in Fig. 5 shows $\Im m U_{opt}$ versus the kinetic in-medium energy E_{kin} at saturation density. At vanishing kinetic energy the imaginary part of the optical potential is rather large

($\simeq -200$ MeV) and consistent with empirical information (error bars) [20]. At high beam energies $\Im m U_{\text{opt}}$ start to decrease again, but remains rather strong. The present estimation seems to be in line with the empirical study of Ref. [25], where $\Im m U_{\text{opt}} = -135$ MeV is essentially independent on the energy in the range from 180 MeV up to $\simeq 2$ GeV.

According to Refs. [19, 20] antiprotons penetrate the nuclear surface up to densities of $\rho \simeq (0.005 - 0.02)\rho_{\text{sat}}$ before annihilation. Therefore, we calculate $\Im m U_{\text{opt}}$ at this low densities, as shown in the main panel of Fig. 5. The filled area indicates the model calculations for matter densities $\rho \simeq (0.005 - 0.02)\rho_{\text{sat}}$. The solid curve shows the model result at an average density of $\rho \simeq 0.01 \rho_{\text{sat}}$. As one can see the NLD model reproduces the data [20] fairly well also at these low densities.

4. Summary and Outlook

In summary, the NLD model, which incorporates on a mean-field level non-linear effects in baryon density and simultaneously in single-particle energy, has been applied to nucleon and antinucleon interactions in nuclear matter. We have shown that due to the explicit energy dependence of the self-energies the proton-nucleus optical potential is very well reproduced. At the same time, the NLD model predicts a much softer real part of the antiproton optical potential at low energies as compared to the Walecka model. We also find a strong decrease of the optical potential with increasing energy. These results are remarkably consistent with available information from reactions involving heavy ion and (anti)proton beams and other studies based on dispersion-theoretical approaches. A comparison with the conventional Walecka model has shown that the main effect responsible for a description of the in-medium (anti)nucleon optical potential originates from the energy dependence of the mean-field, which is absent in standard RMF models. We further estimated the imaginary part of the antiproton optical potential within the NLD model using dispersion relation. The results were in qualitative agreement with the low density data and empirical extrapolations at saturation density. We, therefore, conclude that RMF models may remain a very useful theoretical tool for the description and analysis of the antinucleon interactions in nuclear medium.

The energy dependence of the real and imaginary parts of the antinucleon optical potential, studied in this work, is expected to be important at energies relevant for the PANDA experiment at FAIR. The nuclear compression due to the strong attractive antinucleon mean-field, which significantly differs between the Walecka and the NLD models, and also the very different energy behavior between them will affect the dynamics of antiproton-nucleus reactions. Thus, we expect various observable phenomena at FAIR as important probes for the NLD predictions. For instance, the fragmentation of the excited and radially expanded residual nuclei, where the energy transferred to radial expansion is expected to depend on the degree of compression. Strangeness production of $s = -1$ and especially $s = -2$ hyperons, such as cascade (Ξ) particles, is expected to be medium dependent, in particular close to threshold energies. The associate formation of single- Λ and, in particular, of double-strange hypernuclei is thus supposed to be also model dependent. As an

outlook we conclude the importance and relevance of our results for the future activities at FAIR.

Acknowledgements

This work was supported by HIC for FAIR, DFG through TR16 and by BMBF. We acknowledge useful discussions with A. Larionov.

References

- [1] N. Herrmann, J.P. Wessels, T. Wienold, *Annu. Rev. Nucl. Part. Sci.* 49 (1999) 581.
- [2] B. Blättel, V. Koch, U. Mosel, *Rep. Prog. Phys.* 56 (1003) 1.
- [3] B. ter Haar, R. Malfliet, *Phys. Rep.* 149 (1987) 207.
- [4] K. Weber *et al.*, *Nucl. Phys.* A539 (1992) 713.
- [5] C. Amsler, *Annu. Rev. Nucl. Part. Sci.* 38 (1991) 219.
- [6] W. Cassing, E.L. Bratkovskaya, *Phys. Rep.* 308 (1999) 65.
- [7] S. Teis *et al.*, *Phys. Rev.* C50 (1994) 388.
- [8] E. Hernandez, E. Oset, *Nucl. Phys.* A493 (1989) 453; E. Hernandez, E. Oset, *Nucl. Phys.* A455 (1986) 584-601.
- [9] C.J. Batty, E. Friedman, A. Gal, *Phys. Rep.* 287 (1997) 385.
- [10] \bar{P} ANDA collaboration, hep-ex/0903.3905v1.
- [11] T. Johannsson (\bar{P} ANDA collaboration), XLVIII International Winter Meeting on Nuclear Physics, BORMIO2010 January 25-29, 2010, Bormio, Italy.
- [12] T. Suzuki, H. Narumi, *Nucl. Phys.* A426 (1984) 413.
- [13] H.P. Duerr, *Phys. Rev.* 103 (1956) 469;
J.D. Walecka, *Ann. Phys. (N.Y.)* 83 (1974) 497.
- [14] T. Hippchen *et al.*, *Phys. Rev.* C44 (1991) 1323.
- [15] A.B. Larionov *et al.*, *Phys. Rev.* C80 (2009) 021601(R).
- [16] I.N. Mishustin *et al.*, *Phys. Rev.* C71 (2005) 035201.
- [17] T. Gaitanos, M. Kaskulov, U. Mosel, *Nucl. Phys.* A828 (2009) 9.
- [18] C.J. Horowitz, B.D. Serot, *Nucl. Phys.* A464 (1987) 613.

- [19] P.D. Barnes *et al.*, Phys. Rev. Lett. 29 (1972) 1132;
H. Poth *et al.*, Nucl. Phys. A294 (1978) 435;
C.J. Batty, Nucl. Phys. A372 (1981) 433;
C.-Y. Wong *et al.*, Phys. Rev. C29 (1984) 574.
- [20] E. Friedmann, A. Gal, J. Mares, Nucl. Phys. A761 (2005) 283;
S. Janouin *et al.*, Nucl. Phys. A451 (1986) 541.
- [21] J. Boguta, A.R. Bodmer, Nucl. Phys. A292 (1977) 413;
Y. Sugahara and H. Toki, Nucl. Phys. A579 (1994) 557.
- [22] E.D. Cooper *et al.*, Phys. Rev. C47 (1993) 297.
- [23] T. Maruyama *et al.*, Nucl. Phys. A573 (1994) 653;
P.K. Sahu *et al.*, Nucl. Phys. A672 (2000) 376;
S. Typel, Phys. Rev. C71 (2005) 064301.
- [24] A.B. Larionov, private communication.
- [25] Z. Yu-shun *et al.*, Phys. Rev. C54 (1996) 332.
- [26] J. Rammer, *Quantum Field Theory of Non-Equilibrium States*, Cambridge University Press (July 30, 2007).